European Review for Medical and Pharmacological Sciences 2023; 27: 744-754

Topical silver nanoparticles reduced with ethylcellulose enhance skin wound healing

A.A.H. ABDELLATIF[1,2], F.A. ALHUMAYDHI[3], O. AL RUGAIE[4], N.S. TOLBA[5], A.M. MOUSA[6,7]

[1]Department of Pharmaceutics, College of Pharmacy, Qassim University, Buraydah, Al-Qassim, Saudi Arabia
[2]Department of Pharmaceutics and Pharmaceutical Technology, Faculty of Pharmacy, Al Azhar University, Assiut, Egypt
[3]Department of Medical Laboratories, College of Applied Medical Sciences, Qassim University, Buraydah, Saudi Arabia
[4]Department of Basic Medical Sciences, College of Medicine and Medical Sciences, Qassim University, Unaizah, Saudi Arabia
[5]Department of Pharmaceutics, Faculty of Pharmacy, Sadat City University, Sadat City, Egypt
[6]Department of Basic Health Sciences, College of Applied Medical Sciences, Qassim University, Buraydah, Saudi Arabia
[7]Department of Histology and Cell Biology, Faculty of Medicine, Benha University, Benha, Egypt

Abstract. – OBJECTIVE: Silver nanoparticles (G-AgNPs) improve wound healing by promoting skin cell proliferation and differentiation. Therefore, G-AgNPs could act as drug carriers and wound healers in biomedicine. The current study aimed to improve skin wound healing using natural, safe G-AgNPs.

MATERIALS AND METHODS: The G-AgNPs were reduced with ethylcellulose (EC) and incorporated into an oil-in-water cream base. The size, charges, and wavelength were used to characterize the prepared G-AgNPs. Further, the transmission electron microscope (TEM) and the scanning electron microscope (SEM) were used to provide the shape of G-AgNPs. Moreover, the skin wound healing was evaluated with the appropriate histopathological techniques in a mouse model with skin injury to prove the curative effects of G-AgNPs which was conducted for 15 days on 45 adult male albino rats. The effectiveness of G-AgNPs-EC cream for treating surgical skin wounds was assessed by histopathological (HP) examination of hematoxylin and eosin (H&E) stained sections.

RESULTS: The produced G-AgNPs-EC showed a size of 183.9 ± 0.854 nm and a charge of -14.0 ± 0.351 mV. UV-VIS spectra showed a strong absorption of electromagnetic waves in the visible region at 381 nm. Furthermore, the TEM and SEM showed rounded NPs in nano size of the prepared G-AgNPs-EC. The G-AgNPs cream was pivotal in enhancing wounds' healing properties, improving the formation of wound granulation tissue, and enhancing the proliferation of epithelial tissue in rats.

CONCLUSIONS: The current study showed that G-AgNPs-EC is a new skin wound healer that speeds up healing.

Key Words:
Ethylcellulose, Wound healing, Silver nanoparticles, Antiproliferative, Anti-inflammatory effect.

Introduction

Wounds are physical, chemical, or mechanical tissue damage. So they are sensitive to bacterial infections that inflame and destroy skin tissues[1]. Both diabetic and healthy individuals struggle against the severe problem of wound healing and the prevention of proper skin wound healing[2]. Silver sulfadiazine or pentoxifylline may induce toxicity when treating skin wounds[3]. A constant quest for new materials and procedures may lower the danger of scar development and delay wound healing[4]. Therefore, there is an urgent need to discover new ways to promote and improve the process of skin wound healing and care[5].

Silver has been used for treating many diseases, such as wounds, pleurodesis, and some other dermatological disorders[6]. Herein, silver nanoparticles (G-AgNPs) showed remarkable physicochemical properties over the traditional medications as an alternative and outstanding option compared to the other antimicrobials[7]. Moreover, the ef-

Corresponding Authors: A.A.H. Abdellatif, Ph.D; e-mail: a.abdellatif@qu.edu.sa
Fahad A. Alhumaydhi, Ph.D; e-mail: f.alhumaydhi@qu.edu.sa

fects of G-AgNPs could be caused by blocking and altering the cell wall's breathing enzyme pathways, which results in their tremendous antimicrobial effects. According to Modak and Fox8, the AgNPs have potential pro-healing properties and antibacterial activities. G-AgNPs are alternative NPs to avoid the toxicity of synthetic AgNPs. Recent studies[4] reported the role of G-AgNPs in skin wound healing.

In contrast, numerous studies[9] mentioned that AgNPs had been used as a mouthwash (with 5 nm size) following oral surgery due to their multiple biological activities, such as antibacterial and wound healing properties. Recently, cryogen has been tagged with AgNPs and biodegradable gelatin for treating skin burns caused by Pseudomonas aeruginosa[10]. Furthermore, using guar gum and curcumin to stabilize AgNPs hydrogels improves their characteristic wound-healing power[11].

This study aimed to improve skin wound healing by using a natural, safe method of G-AgNPs. The G-AgNPs were reduced with ethylcellulose (EC) and incorporated into an oil-in-water cream base. The G-AgNPs' size and charges were measured using the zetasizer-nano instrument, and their wavelength was measured by the UV/VIS Spectrophotometer. Fourier transform infrared (FTIR) was used to prove the G-AgNPs' compatibility with the cream. In contrast, the transmission electron microscope (TEM) and scanning electron microscope (SEM) results confirmed the shape of the G-AgNPs. Further, the formulated G-AgNPs were tested physically, and skin wound healing was evaluated with the appropriate histopathological techniques in a mouse model with skin injury to prove the curative effects of G-AgNPs against skin wound injury.

Materials and Methods

Materials and Study Design

Sodium chloride, sodium dihydrogen phosphate, disodium hydrogen phosphate, sodium hydroxide, nitric acid, and hydrochloric acid were purchased from Merck Company (Darmstadt, Germany). 2,2-diphenyl-1-picrylhydrazyl (DPPH) and MTT assay reagent were purchased from Sigma Aldrich Company (Steinheim, Germany). Cytokine-specific enzyme-linked immunosorbent assays were purchased from Santa Cruz Biotechnology Inc. (Bergheimer, Heidelberg, Germany). TNF-α (ABIN6574141) was purchased from antibodies-online GmbH (Aachen, Germany).

The experiment of the current study was conducted for 15 days on 45 adult male albino rats (aged six weeks and weighing 153-198 gm). Under a light-dark cycle of 12 h, all rats were given a diet consisting of chow and free access to running water. This study was agreed upon by the Research Ethics committee of Qassim University (21-10-06), following the "National Research Council Guide for the Care and Use of Laboratory Animals" (NIH Publication No. 8023, revised 1978)[12]. The rats were divided into three equal groups (15 rats for each control, sham, and G-AgNPs-EC). The skin of the control group (G1) was shaved and topically treated with distilled water, and the sham (placebo) group, known as G2, had surgical trauma and was treated topically with vaseline. In contrast, the skin of the third group (G3) was surgically wounded and treated with G-AgNPs-EC topical cream. To prepare the surgical site, the middle portion of each back skin was shaved and sterilized with 65% ethyl alcohol. On day zero, G2 and G3 developed wounds on their skin. Finally, the vaseline and G-AgNPs-EC cream were applied topically to the skin wounds twice daily using cotton swabs on days zero, 4, 10, and 1513.

A full-thickness excisional skin punch biopsy (0.8 cm) was obtained from the rat dorsal skin under the local anesthetic condition at the end of days 4 (subgroups A), 10 (subgroups B), and 15 (subgroups C). A histopathological (HP) investigation of skin sections was carried out using the hematoxylin and eosin (H&E) stains to evaluate the effectiveness of G-AgNPs-EC cream for surgical skin wound treatment according to the previous study by Norman et al[14].

Synthesis of G-AgNPs-EC

G-AgNPs16,17 were prepared and stabilized with EC using the previously reported technique by Abdellatif et al15. Simply EC standard 1% solution was prepared in distilled water, then AgNO3 aqueous solution 1 mM was prepared and adjusted for pH (8.2) and ionic strength using 1 mL Mole NaOH. The prepared AgNO3 solution was heated to boil over a hot plate and kept stirring after adding 2 mL of the prepared EC solution. After 25 min, the dark brown solution's color indicated the formation of G-AgNPs-EC. Finally, the solution was cooled to 25°C and purified from large particulates via centrifugation at 1,500 rpm to extract the NPs Field concrete aggregates[18].

Size and Charge

The size and charge of the generated G-AgNPs-EC were measured using a Malvern Zetasizer Nano Z.S. (Malvern Instruments GmbH, Herrenberg, Germany)[15]. Data were presented as the average of three measurements from the same NPs batch.

UV-VIS Spectrophotometry

To confirm the formation of G-AgNPs synthesis, a UV-VIS scanning and a double beam spectrophotometer (PerkinElmer, lambda 25, UV-VIS Spectrophotometer, Waltham, MA, USA) were employed in the range of 300-600 wavelengths compared with a control solution of AgNO3.

G-AgNPs-EC Morphology

The G-AgNPs-EC were dried overnight on carbon-coated copper grids. A transmission electron microscope [(TEM), JEM-1230, Jeol, Tokyo, Japan] and a scanning electron microscope [(SEM) JEOL JFC-1300, Jeol, Tokyo, Japan] were utilized to examine the morphology of the G-AgNPs-EC[19,20]. The surplus solution was absorbed using filter paper, and the copper grids were washed twice in distilled water for 3-6 sec. The samples were treated with 2% aqueous uranyl acetate, dried at room temperature, and displayed to discover the G-AgNPs-EC solutions on the copper grids[19].

Formulation of G-AgNPs-EC Cream

Oil-in-Water topical cream was prepared following the method of Logan et al[21]. The ingredients (stearic acid, potassium hydroxide, glycerin, propylparaben, and methylparaben) were gradually mixed before being heated to 67°C. To achieve a topical formulation containing 2% G-AgNPs-EC, the congealed emulsion was chilled to a temperature of 52°C while continuously stirring and agitated until it became homogenous.

Characterization of G-AgNPs-EC Cream

The cream was evaluated for emulsion formula according to Dingcong[22]. 1 g of the created cream was mixed with 50 mL of Millipore water at 600 rpm for 10 min, and the cream solubility in water indicates the emulsion type. The visual appearance was used to determine the cream's homogeneity. Additionally, a small part of the cream was lightly rubbed between the fingertips (thumb and index) to evaluate the performance of the newly created cream loaded with G-AgNPs-EC23. A pH meter was utilized to determine the cream's pH value (Ohaus Corporation, model: ST300, USA) as described in a previously published procedure[24].

Clinical Scoring of the G-AgNPs-EC Cream Effects on Skin Wound Severity

Photographs from the skin wound of all rats were obtained to assess the various stages of wound healing at the end of days 4, 10, and 15. Then, the scale bar of the Image J software program was used to measure the surface area of skin wounds to estimate the efficacy of G-AgNPs-EC loaded cream for skin wound healing.

Histopathological Investigation of G-AgNPs-EC Cream Effects on the Activity of Wound Healing

Skin samples were taken from all groups by a skin punch biopsy (0.8 cm^2) on days 4, 10, and 15. The samples were fixed in 10% formalin and processed to obtain thin paraffin sections (5 µm) stained with H and E. The slides were examined under a light microscope for HP research to evaluate the parameters of skin wound changes (the number of inflammatory cells, the granulation tissue formation score, and the epidermal re-epithelialization score). The scoring system was rated from 1 to 4 (1=no change, 2=mild, 3=moderate, and 4=severe) following the scoring system of Sedighi et al[25].

Statistical Analysis

The mean (M±SD) of the surface area and parameters of skin wound healing (number of inflammatory cells, amount of granulation tissue formation, and the degree of epidermal re-epithelialization) were statistically analyzed by the SPSS program version 26 (IBM Corp., Armonk, NY, USA). The tested data normality by using skewness and Kurtosis tests revealed normal data distribution, and One-way ANOVA followed by an LSD test was applied to compare the groups. The Student's *t*-test was applied to compare the two groups. p-value ≤ 0.05 is statistically significant[26].

Results

Characterization of The Topical Cream Containing G-AgNPs-EC

The produced G-AgNPs-EC were measured for their size and zeta potential, 183.9±0.854 nm in size (Figure 1A) and a charge of -14.0±0.351 mV, respectively (Figure 1B). The stability of the created dispersion was indicated by a high value for the zeta potential. It was clear from the UV-VIS spectra that AgNPs showed a strong absorption of electromagnetic waves in the visible region due

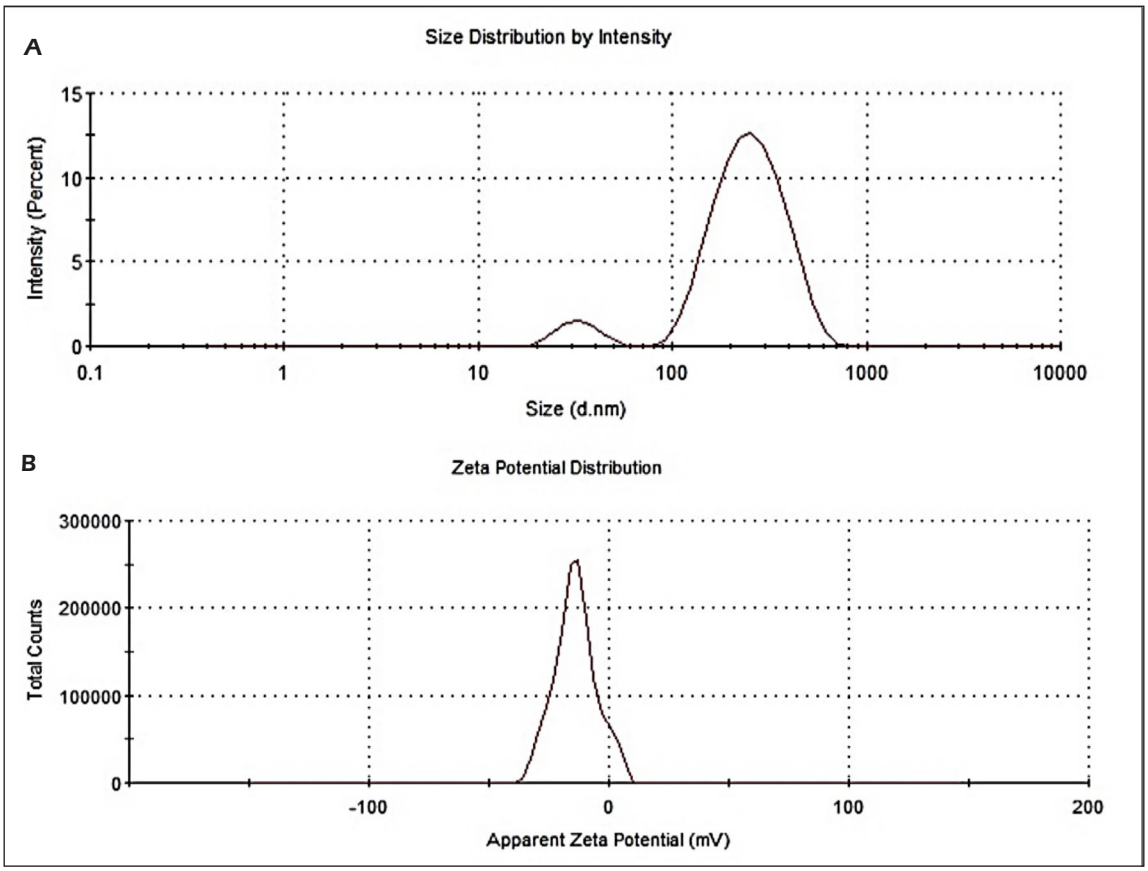

Figure 1. Size distributions (**A**) and zeta-potentials (**B**) for green synthesized silver nanoparticles reduced with ethylcellulose (G-AgNPs-EC).

to the effects of surface Plasmon resonance. The UV-spectroscopy recorded a maximum wavelength of 381 nm for G-AgNPs-EC, indicating the successful preparation of the G-AgNPs-EC27. The current study showed the ability of ECs to coat NPs, preventing their aggregation and increasing their physical stability[28].

AgNPs were visible in the UV-VIS spectra owing to the surface Plasmon resonance phenomenon, which absorbed the electromagnetic radiation in the visible range (Figure 2). The G-AgNPs-EC had a maximum UV-spectroscopy wavelength of 381 nm.

The SEM and TEM revealed that the G-AgNPs-EC particles' morphology showed that the G-AgNPs-EC are non-aggregated and spherical. The images of G-AgNPs-EC are demonstrated in Figure 3. Average sizes of G-AgNPs-EC were less than 100 nm but showed as spots as shown in the TEM image (Figure 3A). G-AgNPs-EC showed a fiber-like structure due to the nature of EC. Furthermore, the SEM image showed nanostructured particles (Figure 3B). After that, the metallic cations appeared consistently in the form of AgNPs[29]. The mobility of metallic cations would diminish due to these interactions, which would also stop the formation of oversized particles and stabilize metallic nanoparticles[28].

The base cream was white with a shiny pearly look, was not greasy, and was easily rinsed with water. Further, upon rubbing, the cream was miscible with water and quickly absorbed by the skin, while the cream containing G-AgNPs-EC as an active ingredient was black-brown, had a moderate natural shine, and was very smooth. Additionally, all particles of the G-AgNPs-EC were dispersed entirely and distributed in one phase within the cream. At the same time, they gradually faded away through the skin layers and improved their appearance. Furthermore, the vanishing cream was mixed with 20 ml of water, homogeneously stirred for 10 min, and appeared as one phase without separation, confirming that the cream was O/W.

Table I. Formulation and characterization of the G-AgNPs-EC cream.

Homogeneity	Viscosity (cPs)	pH	Formula
Good	981±130	6.1±0.21	Base cream
Very good	977±120	5.8±0.34	G-AgNPs-EC cream

G-AgNPs-EC: silver nanoparticles-ethylcellulose.

On the other hand, the studied pH, viscosity, and homogeneity of the G-AgNPs-EC cream exhibited that the pH of the cream base and the G-AgNPs-EC cream were 6.1±0.21 and 5.8±0.34, respectively (Table I). The base and G-AGNPs-EC cream showed pH values comparable to the skin values indicating that these compositions are suitable for use on human skin. Moreover, the G-AgNPs-EC creams had a higher viscosity than the vanishing creams base, which showed a viscosity of 981±130 and 977±120 for the base and G-AgNPs-EC creams, respectively (Table I).

Clinical Evaluation of the Skin Wound's Severity on Days 4, 10, and 15

Figure 4 shows the surface areas of skin wounds measured after receiving vaseline or G-AgNPs-EC cream on days 4, 10, and 15. The wound healing activity in the subgroups of G-AgNPs-EC cream (GC1, 2, and 3) was statistically significant compared to the sham subgroups (GB1, 2, and 3). The wounds that received the G-AgNPs-EC cream on day 4 (the GC1 subgroup) showed mild reductions in the wound surface areas (49.00±2.449 mm^2) compared to the wounds' surface areas (58.80±1.304 mm^2) that received vaseline on the same day (GB1 subgroup). In contrast, the GC2 and 3 subgroups showed significant reductions in the wounds' surface areas on days 10 (27.80±2.588 mm^2) and 15 (9.00±1.225 mm^2) compared to the GB2 (50.60±1.140 mm^2) and GB3 (30.80±2.387 mm^2) subgroups, respectively, indicating the powerful healing ability of the G-AgNPs-EC cream on the same days.

Histopathological Scoring of the Wound Lesions on Days 4, 10, and 15

As depicted in Figure 5, the control subgroups (GA1, 2, 3) on days 4, 10, and 15 revealed standard skin structure, while the sham subgroups (GB1)

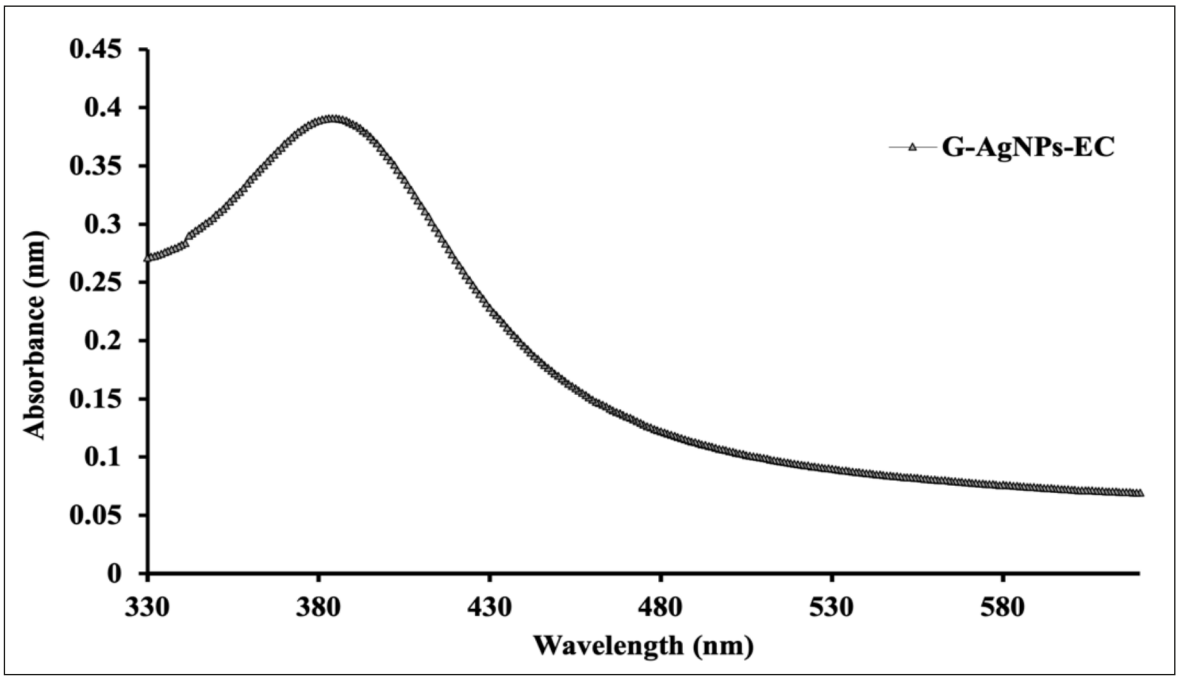

Figure 2. UV-VIS spectra for G-AgNPs-EC.

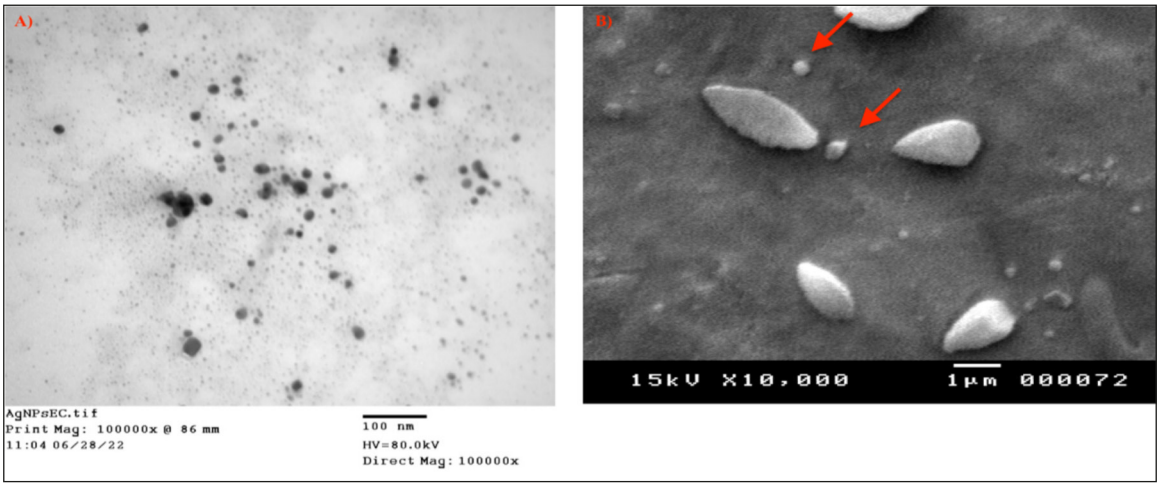

Figure 3. Image of AgNPs-EC using the TEM (**A**) and Image of AgNPs-EC using the SEM (**B**).

exhibited wound gaps, partially filled dermis with necrotic tissue, exudate and inflammatory cells on day 4. In contrast, the sham subgroup on day 10 (GB2) showed a crust covering the wound with intense inflammatory cells and hemorrhagic wound granulation tissue, while the sham subgroup on day 15 (GB3) showed mild inflammation and hemorrhagic injury granulation tissue and epidermal re-epithelialization. At the same time, the G-AgNPs-EC subgroups revealed improvement

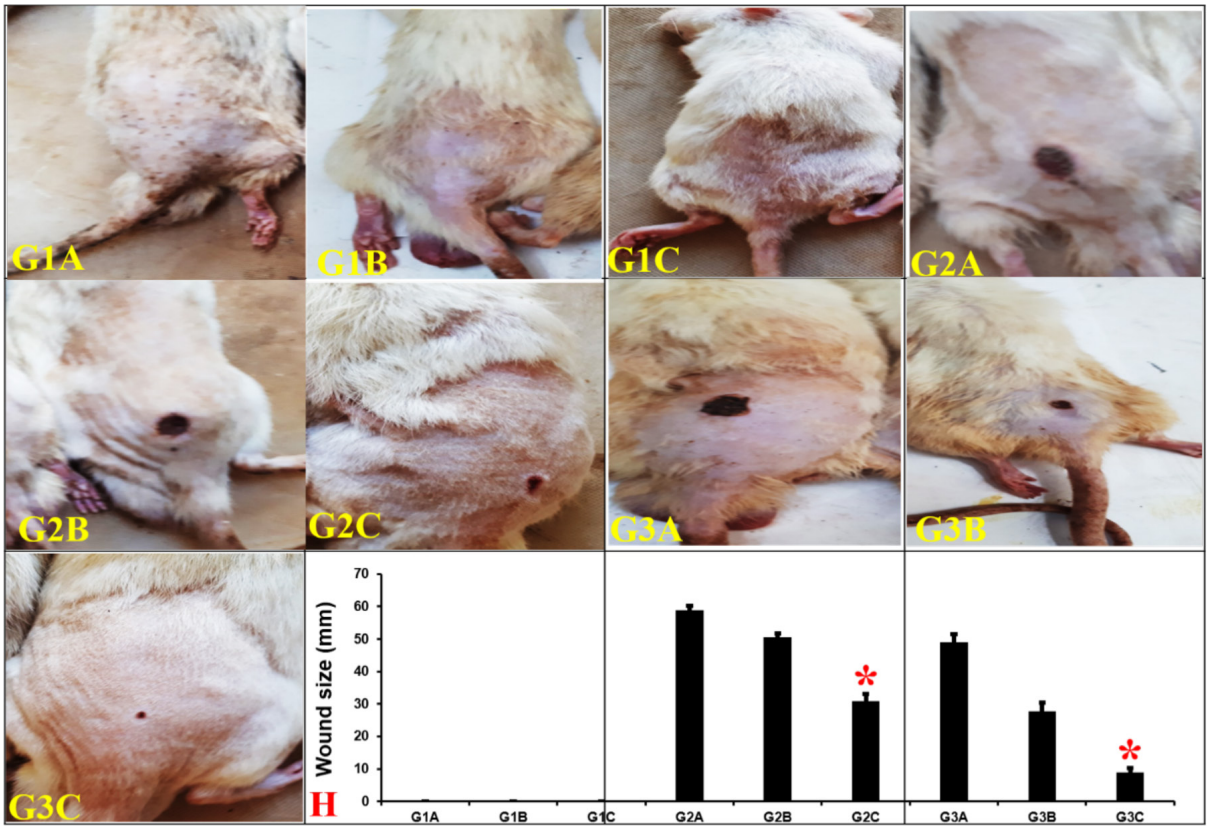

Figure 4. Skin photographs representing all groups, showing the average surface areas of skin wounds on days 4, 10, and 15. Data are expressed as mean±SD in the histogram (**H**). *G2C reveals a significant difference *vs.* G2A and G2B ($p \leq 0.05$).

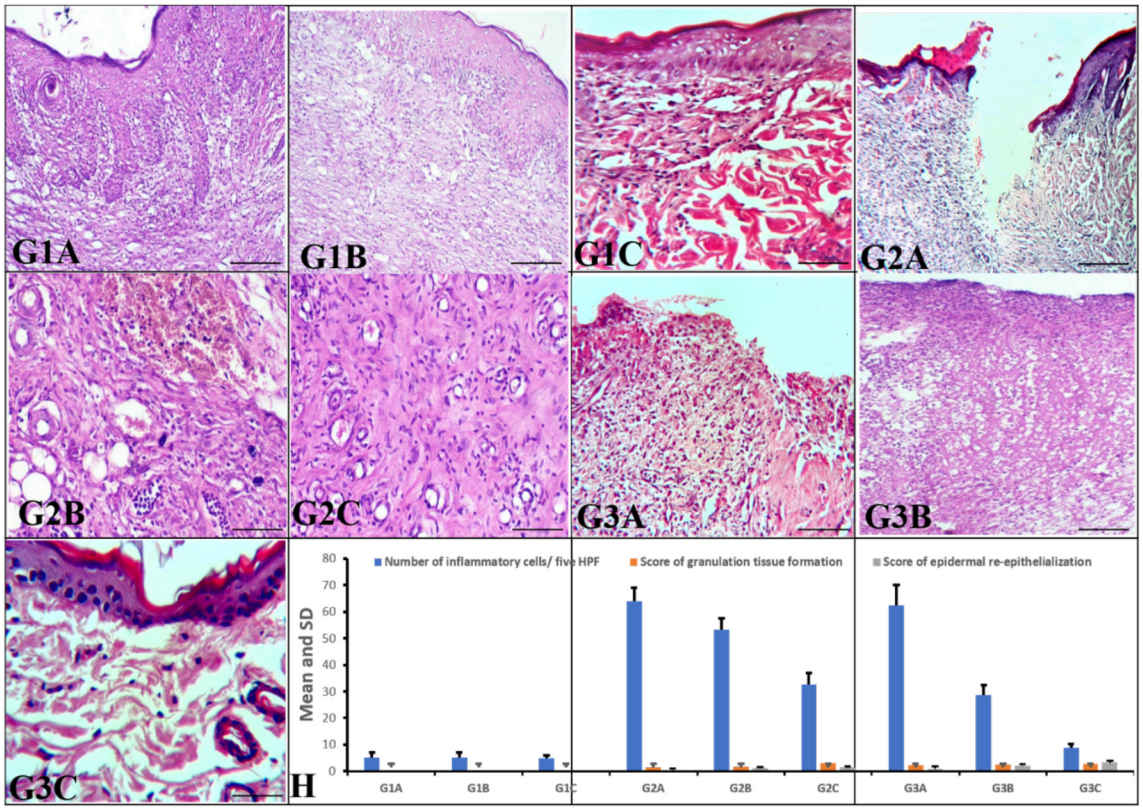

Figure 5. The wound healing scores (the numbers of inflammatory cells, granulation tissue formation, and epidermal re-epithelialization) of all groups on days 4, 10, and 15. The magnification power of **G1A**, **G1B**, **G2A**, **G3A**, and **G3B** is 100X and the scale bar is 100 μm, while they are 200X and 50 μm in **G1C**, **G2B**, and **G2C**. Data are expressed as mean±SD in the histogram (**H**). ***G2C** reveals a significant difference *vs.* G2A and **G2B** ($p \leq 0.05$).

in the scores of wound healing signs (minimal inflammatory cells infiltration and new granulation tissue formation) in the GC2 subgroup compared to the GB2 subgroup on day 10 and a significant increase in the scores of granulation tissue formation and epidermal re-epithelialization in the GC3 subgroup that displayed high reepithelization scores compared to the GB3 subgroup on day 15. Additionally, statistical analysis of the wounds' healing scores (H) showed a significant decrease in the inflammatory cells infiltration scores of the GC2 subgroup compared to the GB2 subgroup on day 10 and a substantial increase in the granulation tissue formation and epidermal re-epithelialization scores among the GC3 subgroup compared to the GB3 subgroup on day 15.

Discussion

Plant extracts have been considered safe and nontoxic nanoparticles, whereas green synthesis provides numerous advantages over conventional physical and chemical processes regarding economic and environmental aspects. Besides, the EC is a non-toxic, eco-friendly reagent which could be used to synthesize G-AgNPs[30,31]. Our previous[15] research demonstrated the adaptability and usefulness of cellulosic polymers for the practical synthesis of G-AgNPs. In terms of superior physical stability, size and charge were considered factors affecting the stability of the formed AgNPs. The obtained AgNPs were of uniform size and stable charges (i.e., the particles of higher charge and small size, the greater stability of its complexes)[43]. EC showed excellent results for incredible antioxidant and antibacterial activity15. Therefore, the EC was mainly selected for the current study. The G-AgNPs-EC was synthesized by reducing silver nitrate with ethylcellulose, which works as a reducing agent and stabilizing component for the G-AgNPs synthesis with low aggregations[15,32]. Ethylcellulose has a reduction power which is the hydroxyl groups that can reduce silver nitrate into AgNPs-EC. The negatively charged EC attaches the positively charged Ag cations to polymeric chains and reduces the

excited facilitating groups. Therefore, the physical results of the G-AgNPs-EC cream agreed with the previously reported results by Abdellatif et al33 and Santini et al[34].

In the current study, synthesizing the G-AgNPs-EC cream involves two steps: atom creation and polymerization[35,36]. The determined size by the TEM was noticeably smaller than that measured by the Zetasizer Nano approach (Dynamic light scattering-based techniques – DLS), and this behavior has been observed by numerous researchers[19,37,38]. Generally, the TEM pictures reflect the metallic center of particles, as TEM demonstrated only the metal core of the NPs3[9]. Furthermore, the DLS-based measurement relies on the mean hydrodynamic diameter and tiny aggregates in nano-suspension, affecting the size and distribution of the G-AgNPs-EC15. The results of both TEM and SEM confirmed the DLS results of the NP size (39.36 nm), which was smaller than the DLS, and are consistent with those observed by the DLS and SEM[19,40,41]. Besides, the observed wavelengths show that the AgNPs have been successfully prepared[27]. A single absorption peak for G-AgNPs-EC preparation revealed that the AgNPs had a symmetrical shape[42].

Like our previous work43, the present work proved the safety and nontoxicity of the G-AgNPs-EC concentration in normal cells. These results are in accordance with the results of Fehaid and Taniguchi44. They mentioned that the broad width of nanoparticles makes them nontoxic compared to normal cells as the G-AgNP size quickly ionized the 10 nm particles, releasing cell-toxic Ag+, and reducing cytotoxicity. Endocytosis can be used for intracellular absorption of 150 nm particles and when they are stored in endosomes, they are not easily ionized and have minimal cytotoxic effects.

The creams were homogeneous, consistent, without gritty particles, and free of particle debris upon visual examination. Besides, the current study data revealed a uniform, smooth cream without visible particles indicating the efficient degree of cream penetration and suggesting the improvement of skin diseases in short periods by topical application of G-AgNPs-EC cream. Similarly, adding NPs containing antioxidants can improve the skin's smoothness, barrier function, and appearance[45]. Additionally, the obtained pH, homogeneity, and viscosity results of the current study proved the suitability of G-AgNPs-EC formulations for topical and transdermal delivery, which agreed with the reported data by Abdellatif and Tawfeek[46], which suggests the valuable role of G-AgNPs-EC topical therapy for the treatment of numerous skin disorders.

At the same time, the HP results of the current study exhibited that the surface areas of skin wounds in GC1, 2, and 3 subgroups (topically received G-AgNPs-EC cream) showed significant reductions compared to the wounds' surface areas of the sham subgroups (GB1, 2, and 3), which typically received vaseline on days 4, 10 and 15, indicating the powerful healing ability of the G-AgNPs-EC cream for various stages of skin wounds. Additionally, the G-AgNPs-EC subgroups revealed noticeable improvement in the wound healing scores (reduction of inflammatory cells infiltration, increase of granulation tissue formation, and increase of epidermal re-epithelialization) in the GC1, 2, and 3 subgroups compared to the GB1, 2, and 3 subgroups on days 4, 10 and 15, displaying the adequate healing power of the G-AgNPs-EC cream on skin wounds.

The obtained HP results have agreed with the findings of many researchers[43,47,48] who mentioned that the generation of reactive oxygen species (ROS) could provoke the antibacterial activity of capped AgNPs. Furthermore, the mannan sulfate-capped AgNPs downregulate TNF-α and IL-6 expression and production in the albino rats, indicating the anti-inflammatory activity of AgNPs.

Conclusions

Using cellulosic polymers in a straightforward process produced stable non-aggregated G-AgNPs-EC formulations due to their effective coating by UV-VIS absorption spectra. Furthermore, the geometric nanoparticle size and the zeta potential were enough to stabilize the incorporated G-AgNPs-EC cream (in vanishing oil in water) with a homogenous compatible cream for easy application on the rat's skin wounds. Additionally, the formulated G-AgNPs-EC revealed a promising activity of skin wound healing with minimal inflammatory cells infiltration, mature collagen fibers formation, and complete skin wound re-epithelialization. Consequently, the current study revealed that G-AgNPs-EC could be considered a novel wound-healing product, which has a powerful implication for wound healing treatment.

Conflict of Interest

The Authors declare that they have no conflict of interests.

Informed Consent

Not applicable.

Funding

The authors gratefully acknowledge Qassim University, represented by the Deanship of Scientific Research, on the financial support for this research under the number (10108-pharmacy-2020-1-3-I) during the academic year 1441 AH/ 2020 AD.

Ethics Approval

This study was agreed upon by the Research Ethics committee of Qassim University (21-10-06), following the "National Research Council Guide for the Care and Use of Laboratory Animals" (NIH Publication No.8023, revised 1978).

References

1) Hurlow JJ, Humphreys GJ, Bowling FL, McBain AJ. Diabetic foot infection: A critical complication. Int Wound J 2018; 15: 814-821.
2) Yu R, Zhang H, Guo B. Conductive Biomaterials as Bioactive Wound Dressing for Wound Healing and Skin Tissue Engineering. Nanomicro Lett 2021; 14: 1.
3) Shende P, Gupta H. Formulation and comparative characterization of nanoparticles of curcumin using natural, synthetic and semi-synthetic polymers for wound healing. Life Sci 2020; 253: 117588.
4) Naraginti S, Kumari PL, Das RK, Sivakumar A, Patil SH, Andhalkar VV. Amelioration of excision wounds by topical application of green synthesized, formulated silver and gold nanoparticles in albino Wistar rats. Mater Sci Eng C Mater Biol Appl 2016; 62: 293-300.
5) Farghaly Aly U, Abou-Taleb HA, Abdellatif AA, Sameh Tolba N. Formulation and evaluation of simvastatin polymeric nanoparticles loaded in hydrogel for optimum wound healing purpose. Drug Des Devel Ther 2019; 13: 1567-1580.
6) Antonangelo L, Vargas FS, Teixeira LR, Acencio MM, Vaz MA, Filho MT, Marchi E. Pleurodesis induced by talc or silver nitrate: evaluation of collagen and elastic fibers in pleural remodeling. Lung 2006; 184: 105-111.
7) Lok CN, Ho CM, Chen R, He QY, Yu WY, Sun H, Tam PK, Chiu JF, Che CM. Silver nanoparticles: partial oxidation and antibacterial activities. J Biol Inorg Chem 2007; 12: 527-534.
8) Modak SM, Fox CL. Binding of silver sulfadiazine to the cellular components of Pseudomonas aeruginosa. Biochem Pharmacol 1973; 22: 2391-2404.
9) Moaddabi A, Soltani P, Rengo C, Molaei S, Mousavi SJ, Mehdizadeh M, Spagnuolo G. Comparison of antimicrobial and wound-healing effects of silver nanoparticle and chlorhexidine mouthwashes: an in vivo study in rabbits. Odontology 2022; 110: 577-583.
10) Huang Y, Bai L, Yang Y, Yin Z, Guo B. Biodegradable gelatin/silver nanoparticle composite cryogel with excellent antibacterial and antibiofilm activity and hemostasis for Pseudomonas aeruginosa-infected burn wound healing. J Colloid Interface Sci 2022; 608: 2278-2289.
11) Bhubhanil S, Talodthaisong C, Khongkow M, Namdee K, Wongchitrat P, Yingmema W, Hutchison JA, Lapmanee S, Kulchat S. Enhanced wound healing properties of guar gum/curcumin-stabilized silver nanoparticle hydrogels. Sci Rep 2021; 11: 21836.
12) Mousa AM, Soliman KEA, Alhumaydhi F, Almatroudi A, Al Rugaie O, Allemailem KS, Alrumaihi F, Khan A, Rezk MY, Aljasir M, Alwashmi ASS, Aba Alkhayl FF, Albutti AS, Seleem HS. Garlic Extract Alleviates Trastuzumab-Induced Hepatotoxicity in Rats Through Its Antioxidant, Anti-Inflammatory, and Antihyperlipidemic Effects. J Inflamm Res 2021; 14: 6305-6316.
13) Kianvash N, Bahador A, Pourhajibagher M, Ghafari H, Nikoui V, Rezayat SM, Dehpour AR, Partoazar A. Evaluation of propylene glycol nanoliposomes containing curcumin on burn wound model in rat: biocompatibility, wound healing, and anti-bacterial effects. Drug Deliv Transl Res 2017; 7: 654-663.
14) Norman G, Dumville JC, Mohapatra DP, Owens GL, Crosbie EJ. Antibiotics and antiseptics for surgical wounds healing by secondary intention. Cochrane Database Syst Rev 2016; 3: CD011712.
15) Abdellatif AAH, Alturki HNH, Tawfeek HM. Different cellulosic polymers for synthesizing silver nanoparticles with antioxidant and antibacterial activities. Sci Rep 2021; 11: 84.
16) Kolarova K, Samec D, Kvitek O, Reznickova A, Rimpelova S, Svorcik V. Preparation and characterization of silver nanoparticles in methyl cellulose matrix and their antibacterial activity. Japan J Appl Phys 2017; 56: 06GG09.
17) Suwan T, Khongkhunthian S, Okonogi S. Silver nanoparticles fabricated by reducing property of cellulose derivatives. Drug Discov Ther 2019; 13: 70-79.
18) Elbakry A, Zaky A, Liebl R, Rachel R, Goepferich A, Breunig M. Layer-by-layer assembled gold nanoparticles for siRNA delivery. Nano Lett 2009; 9: 2059-2064.
19) Tawfeek HM, Abdellatif AAH, Abdel-Aleem JA, Hassan YA, Fathalla D. Transfersomal gel nanocarriers for enhancement the permeation of lornoxicam. J Drug Del Sci Technol 2020; 56: 33.
20) Sun Q, Cai X, Li J, Zheng M, Chen Z, Yu C-P. Green synthesis of silver nanoparticles using tea leaf extract and evaluation of their stability and antibacterial activity. Colloids Surf A Physicochem Eng Asp 2014; 444: 226-231.

21) Logan RA, Hay RJ, Whitefield M. Antifungal efficacy of a combination of benzoic and salicylic acids in a novel aqueous vanishing cream formulation. J Am Acad Dermatol 1987; 16: 136-138.

22) Dingcong W. A study of identifying the emulsion type of surfactant: volume balance value. J Colloid Interface Sci 2002; 247: 389-396.

23) Carneiro RL, Poppi RJ. Infrared imaging spectroscopy and chemometric tools for in situ analysis of an imiquimod pharmaceutical preparation presented as cream. Spectrochim Acta A Mol Biomol Spectrosc 2014; 118: 215-220.

24) Bonde S, Mavani N, Bonde C. Formulation, Optimization and Evaluation of Organogel for Topical Delivery of Acyclovir. Curr Drug Deliv 2018; 15: 397-405.

25) Sedighi A, Mehrabani D, Shirazi R. Histopathological evaluation of the healing effects of human amniotic membrane transplantation in third-degree burn wound injuries. Comp Clin Pathol 2016; 25: 381-385.

26) Mousa AM, Soliman KEA, Alhumaydhi FA, Almatroudi A, Allemailem KS, Alsahli MA, Alrumaihi F, Aljasir M, Alwashmi ASS, Ahmed AA, Khan A, Al-Regaiey KA, AlSuhaymi N, Alsugoor MH, Aljarbou WA, Elsayed AM. Could allicin alleviate trastuzumab-induced cardiotoxicity in a rat model through antioxidant, anti-inflammatory, and antihyperlipidemic properties? Life Sci 2022; 302: 120656.

27) Hajji S, Salem RBSB, Hamdi M, Jellouli K, Ayadi W, Nasri M, Boufi S. Nanocomposite films based on chitosan–poly(vinyl alcohol) and silver nanoparticles with high antibacterial and antioxidant activities. Proc Safety Envir Prot 2017; 111: 112-121.

28) Liu H, Wang D, Song Z, Shang S. Preparation of silver nanoparticles on cellulose nanocrystals and the application in electrochemical detection of DNA hybridization. Cellulose 2010; 18: 67-74.

29) He J, Kunitake T, Nakao A. Facile In Situ Synthesis of Noble Metal Nanoparticles in Porous Cellulose Fibers. Chemical Materials 2003; 15: 4401-4406.

30) Mtibe A, Mokhothu TH, John MJ, Mokhena TC, Mochane MJ. Fabrication and Characterization of Various Engineered Nanomaterials. Handbook of Nanomaterials for Industrial Applications: A volume in Micro and Nano Technologies 2018; 151-171.

31) De Matteis V, Rizzello L, Ingrosso C, Liatsi-Douvitsa E, De Giorgi ML, De Matteis G, Rinaldi R. Cultivar-Dependent Anticancer and Antibacterial Properties of Silver Nanoparticles Synthesized Using Leaves of Different Olea Europaea Trees. Nanomaterials (Basel) 2019; 9: 1544.

32) Xu Y, Li S, Yue X, Lu W. Review of silver nanoparticles (AgNPs)-cellulose antibacterial composites. BioRes 2018; 13: 2150-2170.

33) Abdellatif AAH, Alawadh SH, Bouazzaoui A, Alhowail AH, Mohammed HA. Anthocyanins rich pomegranate cream as a topical formulation with anti-aging activity. J Dermatolog Treat 2020; 32: 983.

34) Santini B, Zanoni I, Marzi R, Cigni C, Bedoni M, Gramatica F, Palugan L, Corsi F, Granucci F, Colombo M. Cream formulation impact on topical administration of engineered colloidal nanoparticles. PLoS One 2015; 10: 126366.

35) Hebeish AA, El-Rafie MH, Abdel-Mohdy FA, Abdel-Halim ES, Emam HE. Carboxymethyl cellulose for green synthesis and stabilization of silver nanoparticles. Carbohydrate Polymers 2010; 82: 933-941.

36) Goia DV. Preparation and formation mechanisms of uniform metallic particles in homogeneous solutions. J Mat Chem 2004; 14: 451-458.

37) Ong HX, Traini D, Cipolla D, Gonda I, Bebawy M, Agus H, Young PM. Liposomal nanoparticles control the uptake of ciprofloxacin across respiratory epithelia. Pharm Res 2012; 29: 3335-3346.

38) Said-Elbahr R, Nasr M, Alhnan MA, Taha I, Sammour O. Nebulizable colloidal nanoparticles co-encapsulating a COX-2 inhibitor and a herbal compound for treatment of lung cancer. Eur J Pharm Biopharm 2016; 103: 1-12.

39) Fissan H, Ristig S, Kaminski H, Asbach C, Epple M. Comparison of different characterization methods for nanoparticle dispersions before and after aerosolization. Analytical Methods 2014; 6: 7324-7334.

40) Ong HX, Traini D, Cipolla D, Gonda I, Bebawy M, Agus H, Young PM. Liposomal Nanoparticles Control the Uptake of Ciprofloxacin Across Respiratory Epithelia. Pharm Res 2012; 29: 333.

41) Said-Elbahr R, Nasr M, Alhnan MA, Taha I, Sammour O. Nebulizable colloidal nanoparticles co-encapsulating a COX-2 inhibitor and a herbal compound for treatment of lung cancer. Eur J Pharm Biopharm 2016; 103: 1-12.

42) Pal S, Tak YK, Song JM. Does the antibacterial activity of silver nanoparticles depend on the shape of the nanoparticle? A study of the Gram-negative bacterium Escherichia coli. Appl Environ Microbiol 2007; 73: 1712-1720.

43) Abdellatif AAH, Alsharidah M, Al Rugaie O, Tawfeek HM, Tolba NS. Silver Nanoparticle-Coated Ethyl Cellulose Inhibits Tumor Necrosis Factor-alpha of Breast Cancer Cells. Drug Des Devel Ther 2021; 15: 2035-2046.

44) Fehaid A, Taniguchi A. Size-Dependent Effect of Silver Nanoparticles on the Tumor Necrosis Factor alpha-Induced DNA Damage Response. Int J Mol Sci 2019; 20: 1038.

45) Adu-Frimpong M, Firempong CK, Omari-Siaw E, Wang Q, Mukhtar YM, Deng W, Yu Q, Xu X, Yu J. Preparation, optimization, and pharmacokinetic study of nanoliposomes loaded with triacylglycerol-bound punicic acid for increased antihepatotoxic activity. Drug Dev Res 2019; 80: 230-245.

46) Abdellatif AA, Tawfeek HM. Transfersomal Nanoparticles for Enhanced Transdermal Delivery of Clindamycin. AAPS Pharm Sci Tech 2016; 17: 1067-1074.

47) Wilkinson LJ, White RJ, Chipman JK. Silver and nanoparticles of silver in wound dressings: a review of efficacy and safety. J Wound Care 2011; 20: 543-549.

48) Wong KK, Cheung SO, Huang L, Niu J, Tao C, Ho CM, Che CM, Tam PK. Further evidence of the anti-inflammatory effects of silver nanoparticles. Chem Med Chem 2009; 4: 1129-1135.